Terahertz Optomagnetism: Nonlinear THz Excitation of GHz Spin Waves in Antiferromagnetic $FeBO_3$

E. A. Mashkovich,[1,*] K. A. Grishunin,[1,2] R. V. Mikhaylovskiy,[1,3] A. K. Zvezdin,[4,5] R. V. Pisarev,[6] M. B. Strugatsky,[7] P. C. M. Christianen,[1,8] Th. Rasing,[1] and A. V. Kimel[1]

[1]*Radboud University, Institute for Molecules and Materials, 6525 AJ Nijmegen, The Netherlands*
[2]*MIREA—Russian Technological University, Moscow 119454, Russia*
[3]*Department of Physics, Lancaster University, Bailrigg, Lancaster LA1 4YW, United Kingdom*
[4]*Prokhorov General Physics Institute of the Russian Academy of Sciences, Moscow 119991, Russia*
[5]*Moscow Institute of Physics & Technology, Dolgoprudnyi 141700, Russia*
[6]*Ioffe Physical-Technical Institute, Russian Academy of Sciences, 194021 St Petersburg, Russia*
[7]*Physics and Technology Institute, V.I. Vernadsky Crimean Federal University, 295007 Simferopol, Russia*
[8]*High Field Magnetic Laboratory (HFML—EFML), Radboud University, 6525 ED Nijmegen, The Netherlands*

(Received 1 April 2019; published 11 October 2019)

A nearly single cycle intense terahertz (THz) pulse with peak electric and magnetic fields of 0.5 MV/cm and 0.16 T, respectively, excites both modes of spin resonances in the weak antiferromagnet $FeBO_3$. The high frequency quasiantiferromagnetic mode is excited resonantly and its amplitude scales linearly with the strength of the THz magnetic field, whereas the low frequency quasiferromagnetic mode is excited via a nonlinear mechanism that scales quadratically with the strength of the THz electric field and can be regarded as a THz inverse Cotton-Mouton effect. THz optomagnetism is shown to be more energy efficient than similar effects reported previously for the near-infrared spectral range.

DOI: 10.1103/PhysRevLett.123.157202

The development of high-intensity ultrashort laser pulses opened up new pathways to easily access the nonlinear optical regime, where strong light-matter coupling can lead to a plethora of fundamentally new opportunities for light frequency conversion [1–4] and controlling properties of media by light [5–7]. In magnetism these developments led to the establishment of the new research field of ultrafast magnetism [8–10] and to discussions about the potential of femtosecond optical pulses for the fastest and most energy efficient writing of magnetic data [11].

Pioneering studies of nonlinear optical phenomena in magnetics [2,12] pointed out that light can act as an effective magnetic field [13,14] that efficiently aligns spins and induces a magnetization in media [14]. Regarding symmetry, a cross product of the two orthogonal electric field components of circularly polarized light has the same symmetry as a magnetic field aligned along the wave vector of light. Also, linearly polarized light can induce magnetic anisotropy in magnetized media. Phenomenologically, these effects were described in terms of the optomagnetic inverse Faraday and Cotton-Mouton effects. Combining optomagnetism with femtosecond laser pulses yields the fastest ever and therefore unique stimulus in magnetism. Recently, it was argued that far-infrared pulses are the most energy efficient means to control magnetism [15,16]. Despite many experimental and theoretical studies in the visible, near- [17–19], and midinfrared [20], strong coherent nonlinear coupling of spins to THz light was reported exclusively for $TmFeO_3$ [21]. The mechanism of the coupling relied on resonant pumping of Tm^{3+} ions and was only efficient in a narrow 10 K temperature range in the vicinity of a spin reorientation phase transition. Although the inverse Faraday and Cotton-Mouton effects are much more universal—they do not rely on absorption and must be observed in a broad temperature range—optomagnetic phenomena induced by THz light have not been reported yet and their efficiency is still an open question.

Here we report a nonlinear optomagnetic coupling of THz light to spins in a material with no strong spectral features in the THz spectral range and no phase transition. The mechanism appears to be efficient in a broad temperature range. In particular, using a single crystal of the weak ferromagnet $FeBO_3$ we demonstrate that a nearly single cycle THz pulse excites a GHz spin resonance in this antiferromagnet and the observed dependencies on the polarization of the THz pulse, temperature, and external magnetic field indicate that the mechanism can be assigned to the inverse Cotton-Mouton effect [22–24].

$FeBO_3$ is a material with a low absorption coefficient $\sim 80\ cm^{-1}$ [25] in the visible and $\sim 160\ cm^{-1}$ in the THz spectral range. The latter was measured by means of time resolved THz spectroscopy (Fig. S1 [26]). $FeBO_3$ crystallizes in a calcite-type structure with point group $\bar{3}m$. The schematic of the crystal structure is depicted in Fig. 1(a). The spins of the Fe^{3+} ions form two magnetic sublattices with magnetizations $\mathbf{M}_1$ and $\mathbf{M}_2$, respectively. The sublattices are

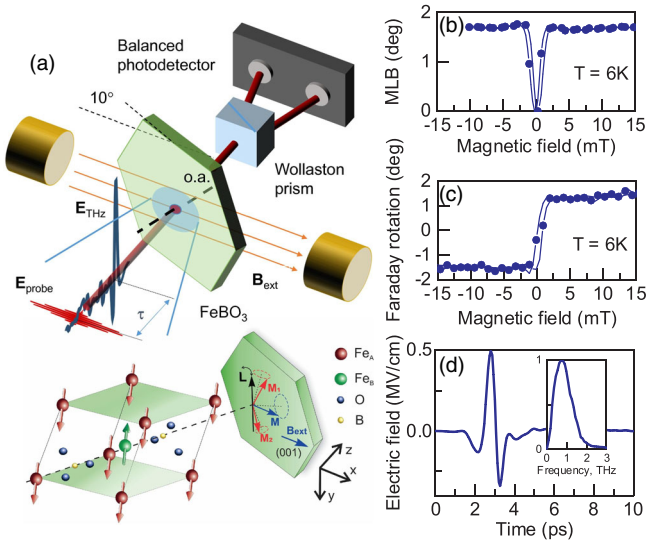

FIG. 1. (a) Schematic of the $FeBO_3$ crystal structure and experimental geometry. THz and optical pulses are focused onto the $FeBO_3$ crystal. The diameter of the probe beam is significantly smaller than that of the THz beam. The external magnetic field $\mathbf{B}_{ext}$ is along the x axis. $\mathbf{L}$ and $\mathbf{M}$ are antiferromagnetic and magnetization vectors, respectively. τ is a controllable time delay between the THz pump pulse and the optical probe pulse. o.a. denotes the optical axis (along the z axis). (b) Ellipticity acquired by linearly polarized light at the wavelength of 800 nm upon propagation along the o.a. as a function of magnetic field applied in the sample plane. (c) Static polarization rotation acquired by linearly polarized light at the wavelength of 800 nm upon propagation through the tilted crystal as a function of magnetic field. The crystal tilt and the orientation of the magnetic field are shown in panel (a). (d) Waveform of the THz electric field and the corresponding Fourier spectrum (inset).

coupled antiferromagnetically and the Néel temperature is ~350 K [35]. Because of the Dzyaloshinskii-Moriya interaction, the spins undergo a slight spin canting of about 1° in the (001) plane, which results in a magnetic moment oriented within this plane, $\mathbf{M} = \mathbf{M}_1 + \mathbf{M}_2$. The magnetization $\mathbf{M}$ and the Néel antiferromagnetic vector $\mathbf{L} = \mathbf{M}_1 - \mathbf{M}_2$ are depicted in Fig. 1(a) [36]. The magnet has a strong "easy-plane" magnetic anisotropy so that both $\mathbf{M}$ and $\mathbf{L}$ lie in the (001) plane. The anisotropy field in the (001) plane is negligible, being of the order of 0.02 mT. Although the M/L ratio is small, a magnetic field of the order of 5 mT applied in the (001) plane is able to control $\mathbf{L}$ and $\mathbf{M}$, aligning the latter along the field.

The feasibility of controlling spins of an antiferromagnet by light via both linear and nonlinear mechanisms can be seen from the laws of thermodynamics [26]. In particular, it can be shown that, in addition to direct, i.e., linear coupling of the magnetic field of light and the magnetization, light should be able to control spins in an antiferromagnet via a nonlinear mechanism, if the optical susceptibility χ_{kl} depends on $\mathbf{M}$ or $\mathbf{L}$. Note that in a weak ferromagnet, $\mathbf{M}$ and $\mathbf{L}$ are not mutually independent variables and $\mathbf{M}$ can be expressed in terms of the real order parameter $\mathbf{L}$ [30,37]. Hence in the following we assume that χ_{kl} depends on $\mathbf{L}$ only.

If dissipation is neglected, $\chi_{kl} = \chi_{lk}^{*}$ and the optical susceptibility tensor can be expressed as a sum of symmetric and antisymmetric parts $\chi_{kl} = \chi_{kl}^{(a)} + \chi_{kl}^{(s)}$, where $\chi_{kl}^{(a)} = -\chi_{lk}^{(a)}$ and $\chi_{kl}^{(s)} = \chi_{lk}^{(s)}$ [38]. According to Onsager's principle, the antisymmetric part of the optical susceptibility $\chi_{kl}^{(a)}$ is an odd function of $\mathbf{L}$, while the symmetric part $\chi_{kl}^{(s)}$ can depend on $\mathbf{LL}$ or its integer powers [39,40]. The dependence of $\chi_{kl}^{(a)}$ on $\mathbf{L}$ renders direct magneto-optical and inverse opto-magnetic Faraday effects. The dependence of $\chi_{kl}^{(s)}$ on $\mathbf{LL}$ renders direct magneto-optical and inverse opto-magnetic Cotton-Mouton effects. The dependencies of $\chi_{kl}^{(a)}$ and $\chi_{kl}^{(s)}$ on the magnetic order parameters can be verified experimentally. Figure 1(b) shows the magnetic field dependence of the ellipticity acquired by linearly polarized light at a wavelength of 800 nm after propagation through the studied $FeBO_3$ crystal. The ellipticity originates from different refraction coefficients experienced by two mutually orthogonal, linearly polarized light waves propagating in the direction of the detector. The difference is proportional to $\mathbf{LL}$ and the effect is called the magneto-optical Cotton Mouton effect or magnetic linear birefringent (MLB). The field was applied in the (001) plane [along the x axis in Fig. 1(a)] and the probing beam propagated along the [001] crystallographic axis [z axis in Fig. 1(a)]. The observed ellipticity is even with respect to the applied magnetic field and must be assigned to the dependence of $\chi_{kl}^{(s)}$ on $\mathbf{LL}$. Figure 1(c) shows the polarization rotation measured in a similar geometry but for light propagating at a small angle of about 10° with respect to the z axis. The measured field dependence of the polarization rotation is odd with respect to the applied magnetic field, known as the direct magneto-optical Faraday effect that probes $\chi_{kl}^{(a)}$. These static and earlier dynamic [41] experiments clearly show that for light at the wavelength of 800 nm the dependence of $\chi_{kl}^{(a)}$ and $\chi_{kl}^{(s)}$ on the magnetic order parameter results in significant magneto-optical and optomagnetic effects. In general, in the near-infrared and visible spectral ranges, it is expected that the Faraday effect, as the first term in a Taylor series, is stronger than the Cotton-Mouton effect. However, taking into account peculiarities of the electronic structure of matter, in a narrow spectral range the ratio between these two effects can be different [42]. Practically nothing is known about optomagnetic effects in the THz domain. Nonetheless, from a quantum mechanical theory of magneto-optical phenomena developed for the case of rare-earth ions [31], one can anticipate that in dielectric media with no free electrons $\chi_{kl}^{(a)}$ and $\chi_{kl}^{(s)}$ have rather different spectral dependencies at low frequencies of light ω: $\lim_{\omega\to 0}\chi_{kl}^{(a)}(\omega) = 0$ and $\lim_{\omega\to 0}\chi_{kl}^{(s)}(\omega) \neq 0$.

Although similar quantum mechanical calculations of the optical susceptibility for $FeBO_3$ are beyond the scope of this Letter, it is clear that, unlike previous experiments with near-infrared and visible light, in the THz spectral range the efficiency of the inverse Cotton-Mouton effect can be higher than that of the inverse Faraday effect.

To study the effect of THz light on spins in $FeBO_3$, we employed intense THz pulses generated by 100 fs optical pulses from a Ti:sapphire amplifier with an energy of about 4 mJ per pulse. The dynamics was mapped using a probe pulse at the wavelength of 800 nm. The generated THz waveform and corresponding spectrum are depicted in Fig. 1(d). Details of the THz generation technique and the experimental setup are provided in the Supplemental Material [26]. If the THz pulse triggers spin dynamics, it can be translated in the dynamics of the magnetization. $FeBO_3$ has two modes of antiferromagnetic spin resonance: a low frequency quasiferromagnetic mode (q-FM) and a high frequency quasiantiferromagnetic mode (q-AFM) [43,44]. In spherical coordinates, where θ is the angle between $\mathbf{L}$ and the z axis, and ψ is the angle between the x axis and projection of $\mathbf{L}$ on the xy plane, one finds $\mathbf{L} = 2|\mathbf{M}_{1,2}|(\sin\theta\cos\psi, \sin\theta\sin\psi, \cos\theta)$. It means that q-FM and q-AFM modes are seen as oscillations of ψ and θ, respectively.

The THz-induced spin dynamics was probed using the magneto-optical Faraday and Cotton-Mouton effects by measuring the polarization rotation of the linearly polarized probe pulse. A typical time trace of the THz induced dynamics of the polarization rotation measured at $T = 6$ K and at an external magnetic field B_{ext} of 40 mT in $FeBO_3$ is shown in Fig. 2(a). The magneto-optical signal exhibits clear oscillations. After performing a Fourier transform these oscillations show up in the frequency domain as two well-defined spectral bands at very different frequencies of 20 and 480 GHz [Fig. 2(b)]. The measurements for different values of B_{ext} are summarized in Fig. 2(c). The absolute values of the frequencies and the field dependencies are in very good agreement with the two modes of antiferromagnetic resonance in this compound [26,43,44].

Figure 2(d) shows how the Fourier amplitudes of the modes depend on the strength of the THz electric field. The high-frequency q-AFM mode scales linearly (solid blue curve) with the THz electric field. Although there is no considerably strong spectral component of the THz spectrum near the q-FM frequency, this mode is excited rather efficiently and its amplitude (solid red curve) scales quadratically with the THz electric field. It reveals that the mechanism of the excitation is off-resonant and nonlinear.

Figure 3(a) shows how the amplitude of the q-FM mode depends on the azimuthal angle α of the linearly polarized THz pump pulse. The azimuthal angle $\alpha = 0°$ corresponds to the THz polarization in the xy plane, perpendicular to the applied magnetic field. The Fourier amplitude of the q-AFM mode has a maximum when the THz magnetic field is

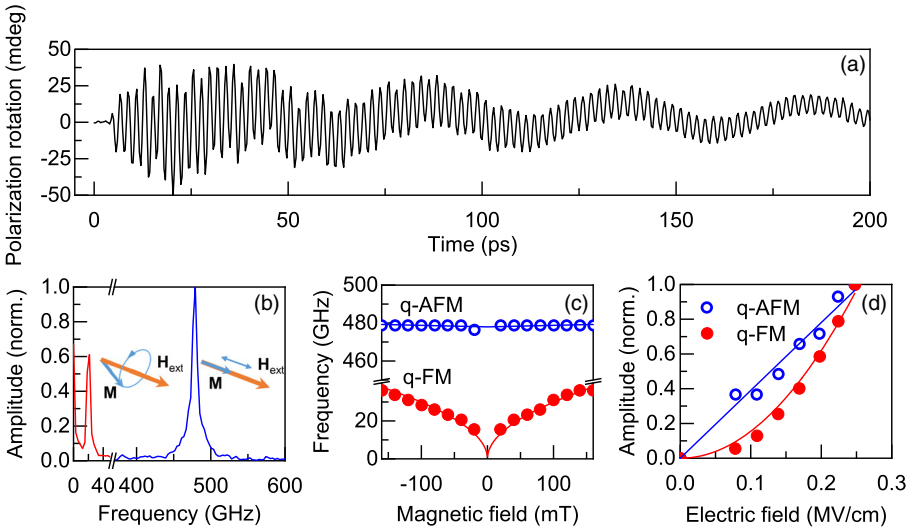

FIG. 2. Optically detected THz-induced spin dynamics in $FeBO_3$. (a) Probe polarization rotation vs time delay τ. Here, the THz pump polarization (direction of the THz electric field) is along the y axis and the optical probe polarization is along the x axis. The crystal was tilted around the y axis over 10°, as shown in Fig. 1(a). $B_{ext} = 40$ mT, $T = 6$ K. (b) Corresponding Fourier spectrum of the waveform shown in (a). Both the high frequency q-AFM and the low frequency q-FM modes of magnetic resonance in $FeBO_3$ are clearly seen. The damping constants are 0.1 and 0.004 for the q-FM and q-AFM modes, respectively. Behavior of $\mathbf{M}$ for q-AFM (longitudinal oscillation) and q-FM (precession) modes are shown as insets next to the corresponding spectral maxima. (c) The dependencies of the q-AFM (open blue circles) and the q-FM mode (closed red circles) frequencies on the external magnetic field. Solid lines are fits based on theoretical dependencies for ω_{AFM} (blue curve) and ω_{FM} (red curve) [26]. (d) The dependencies of the amplitudes of q-AFM (open blue circles) and q-FM (closed red circles) modes on the THz electric field. The blue and red curves correspond to linear and quadratic fits, respectively.

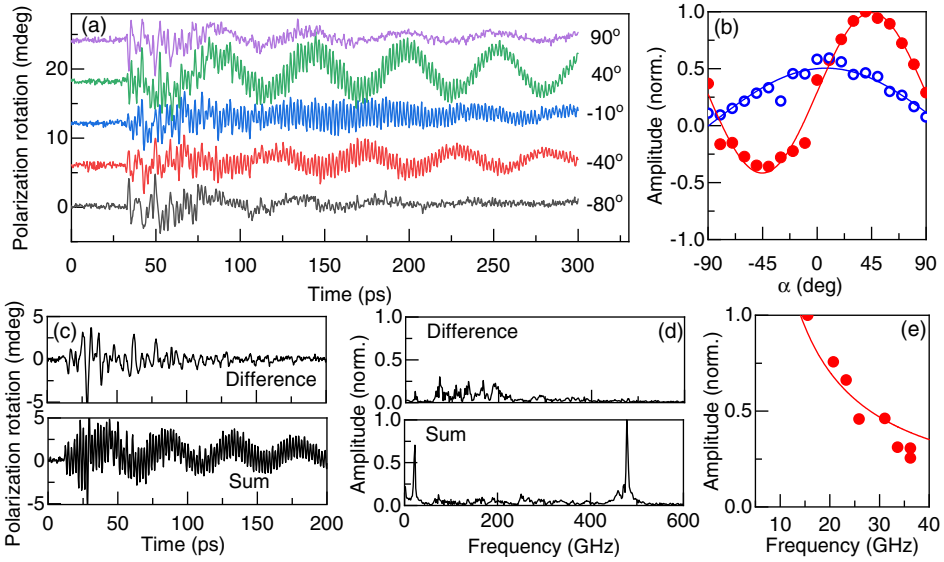

FIG. 3. (a) Optically detected THz induced spin dynamics in $FeBO_3$ measured for different angles α between the THz electric field and the y axis. α is shown near each curve. The crystal was tilted around the y axis over 10°, as shown in Fig. 1(a). $B_{ext} = 40$ mT, $T = 6$ K. (b) Normalized Fourier amplitudes of the q-AFM (open blue circles) and q-FM (closed red circles) modes from panel (a). Change of sign of the amplitude indicates phase changes. The experimental data are fitted by $\sim\cos\alpha$ (blue curve) and $A + B\sin 2\alpha$ (red curve) (c) Waveforms of the magnetization dynamics after deducing the odd (upper panel) and even (lower panel) parts with respect to the polarity of the applied magnetic field ±40 mT. (d) Fourier spectrum of the odd (higher panel) and even (lower panel) waveforms from panel (c). (e) The dependence of the amplitude of the q-FM mode on its frequency. Hyperbolic fit is shown by the red curve.

along the direction of the external magnetic field and the data (open blue circles) are perfectly fitted by $\sim\cos\alpha$ (blue curve) [see Fig. 3(b)]. This azimuthal dependence is in agreement with a mechanism of resonant excitation of the q-AFM mode by the magnetic component of the THz pulse. This mechanism of resonant THz excitation of the q-AFM mode and detection of this mode with the help of magneto-optical effects was in detail described elsewhere [15]. At the same time, the amplitude of the q-FM mode has two extrema at $\alpha = \pm 45°$ and changes polarity around $\alpha = 0°$, being very different from the mechanisms of THz excitation of spin resonances reported before. The experimental data (closed red circles) were fitted by the function $A + B\sin 2\alpha$ (red curve), where A and B are fitting parameters. The fit shows that $A/B < 0.3$, which indicates that the polarization dependent mechanism plays a dominant role in the excitation of the q-FM mode of spin resonance. While the polarization independent excitation of spin oscillations is typical for many different mechanisms of optical control of magnetism [45,46], such a $\sin 2\alpha$ dependence is the same as for the inverse Cotton-Mouton effect reported earlier for $FeBO_3$ for near-infrared light [41]. Substantially different polarization dependencies in Fig. 3(b) show that the resonantly excited magnetic dipole q-AFM mode does not play any role in the nonlinear mechanism of the excitation of the q-FM mode. Therefore, it is reasonable to assume that the nonlinear mechanism must rely on off-resonant excitation of electric-dipole transitions outside the spectrum of the THz pulse.

The experiment shows that a THz pulse triggers harmonic oscillations of spins on a much longer time scale than the pulse duration. Such dynamics in antiferromagnets is described by differential equations for damped harmonic oscillators corresponding to the q-FM and q-AFM modes, respectively [26]. These equations are derived from the Lagrangian, being a solution of the Euler-Lagrange equations for ψ and θ [47]. In the case of normal incidence of the THz pulse and the external magnetic field along the x axis, the torque that triggers the q-AFM mode is $T_{AFM}\sim\dot{H}(t)\cos\alpha$ [30]. For the torque that is generated due to the inverse Cotton-Mouton effect and that triggers the q-FM mode one finds $T_{FM}\sim E^2(t)\sin 2\alpha$ [26]. Here $E(t)$ and $H(t)$ are the electric and magnetic fields of the THz pulse, respectively. A comparison between the outcomes of the model and the experimental results confirms that the q-AFM mode is excited resonantly due to the Zeeman coupling of the THz magnetic field and the sublattice magnetizations, while the q-FM mode is excited due to the mechanism of the inverse Cotton-Mouton effect.

The sum and the difference of the time traces measured at the different polarities of the field $B_{ext} = \pm 40$ mT are shown in Fig. 3(c). Figure 3(d) shows that the dominating part of the THz-induced dynamics is even with respect to the applied magnetic field. For $FeBO_3$ it is known [23] that the q-FM mode is the easiest to detect via the direct magneto-optical Cotton-Mouton effect, i.e., due to the symmetric part of the optical susceptibility. Figures 3(c) and 3(d) show that

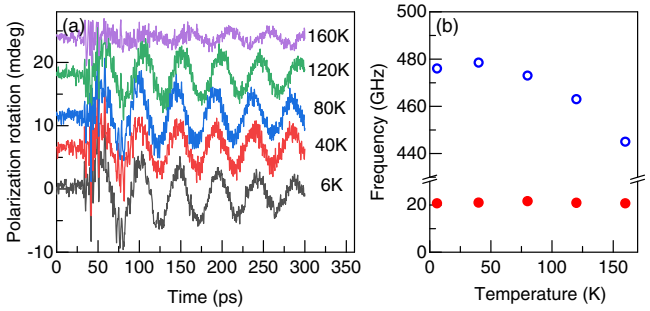

FIG. 4. (a) Optically detected THz induced spin dynamics at different temperatures, indicated near the curves. In the experiment the crystal was tilted around the y axis over 10°, as shown in Fig. 1(a). $B_{ext} = 40$ mT. (b) Frequencies of the q-AFM (open blue circles) and q-FM (closed red circles) modes of the waveforms from panel (a).

the oscillations at the frequency of the q-FM mode are present only in the sum, but not in the difference plot. The signal that appears in the difference is well above the noise level, but its Fourier spectrum [Fig. 3(d)] does not allow ascribing it to spin dynamics. Hence the signal must have a different origin [48]. Similar to Ref. [23], the observed independence of q-FM oscillations on the polarity of the applied magnetic field allows us to confirm that the spin dynamics is excited and detected via the inverse and direct Cotton-Mouton effects, respectively. The detection of magnetization dynamics is discussed in the Supplemental Material [26].

Changing the value of the applied magnetic field one changes the frequency of the q-FM mode. According to Ref. [23], the amplitude of the q-FM mode excited in $FeBO_3$ due to the inverse Cotton-Mouton effect must be inversely proportional to the frequency of the mode itself. This expectation is confirmed experimentally, as shown in Fig. 3(e). The inverse Cotton-Mouton effect in the THz spectral range reported here results in a spin oscillation of the magneto-optical signal with an amplitude of about 10 mdeg for a pump fluence of 0.1 mJ/cm^2. It is remarkable that in earlier reports about the inverse Cotton-Mouton effect in a comparable $FeBO_3$ crystal and for excitation at the photon energy of 1.5 eV, achieving similar amplitudes of the oscillations required much higher pump fluences -10 mJ/cm^2 [23]. Interestingly, even if the THz fluence is 100 times smaller than the fluence of the near-infrared excitation, the average energy of the THz photons is about 1000 times smaller than photon energies in the near-infrared spectral range (1.5 eV). It means that even the far less efficient scattering of THz photons by magnons results in an effect comparable to that for near-infrared light.

Finally, in order to demonstrate that the observed mechanism of THz-induced spin excitation is very different from the one recently reported for $TmFeO_3$ [21], we studied the efficiency of the excitation as a function of temperature, as shown in Fig. 4(a). Although the measurements at temperatures above 160 K are hampered by a reduction of the net Néel vector and consequently of the magneto-optical Cotton-Mouton effect, even these data show that the q-FM mode excitation mechanism remains efficient in a much broader temperature range as compared to the mechanism reported in Ref. [21]. Temperature dependencies of the frequencies of the excited q-FM and q-AFM modes [see Fig. 4(b)] are in a good agreement with previously reported data [49] and this agreement is the best evidence of negligibly small THz-induced heating in our experiment.

In summary, we show that intense THz pulses efficiently trigger spin oscillations corresponding to the two modes of the antiferromagnetic resonance in $FeBO_3$. While the q-AFM mode is resonantly excited by the magnetic field of the incident THz pulse, the q-FM mode is excited off-resonantly and its amplitude scales quadratically with the strength of the THz electric field. The mechanism of the excitation has all the features of the inverse opto-magnetic Cotton-Mouton effect and is at least as efficient as the similar effect in the near-infrared spectral range. Although until now the effect has only been reported for $FeBO_3$, symmetry analysis shows that the corresponding term in the energy of light-matter interaction is not restricted to a specific crystal point group. Similar to the direct Cotton-Mouton effect, the inverse effect must be allowed in materials of other symmetries. The mechanism is also efficient in a broad temperature range and we expect similar nonlinear effects to be found in other magnetically ordered media. This work opens up a previously ignored channel to control spins in magnetically ordered materials in an energy efficient way.

The authors thank T. Toonen, P. Albers, S. Semin, Ch. Berkhout, and F. Janssen for technical support. This work was supported by de Nederlandse Organisatie voor Wetenschappelijk Onderzoek (NWO), European Research Council ERC Grant agreement No. 339813 (Exchange), the Russian Foundation for Basic Research within projects 18-02-40027 and 18-52-53030 as well as HFML-RU/FOM, member of the European Magnetic Field Laboratory (EMFL). The contribution of R. V. P. into the experimental part was supported by the RSF Project No. 16-12-10456. A. K. Z. acknowledges the support by RSF Project No. 17-12- 01333 for theoretical study of spin dynamics.

*Corresponding author.
E.Mashkovich@science.ru.nl

[1] P. A. Franken, A. E. Hill, C. W. Peters, and G. Weinreich, Generation of Optical Harmonics, Phys. Rev. Lett. **7**, 118 (1961).
[2] N. Bloembergen, Nonlinear optics and spectroscopy, Science **216**, 1057 (1982).
[3] U. Simon and F. K. Tittel, in *Experimental Methods in the Physical Sciences* (Elsevier, San Diego, 1997), pp. 231–278.

[4] R. W. Boyd, *Nonlinear Optics*, 3rd ed. (Academic Press, New York, 2008).

[5] F. S. Chen, J. T. LaMacchia, and D. B. Fraser, Holographic Storage in lithium niobate, Appl. Phys. Lett. **13**, 223 (1968).

[6] V. M. Fridkin, *Photoferroelectrics* (Springer Berlin Heidelberg, Berlin, Heidelberg, 1979).

[7] V. F. Kovalenko and É. L. Nagaev, Photoinduced magnetism, Sov. Phys. Usp. **29**, 297 (1986).

[8] E. Beaurepaire, J.-C. Merle, A. Daunois, and J.-Y. Bigot, Ultrafast Spin Dynamics in Ferromagnetic Nickel, Phys. Rev. Lett. **76**, 4250 (1996).

[9] A. V. Kimel, A. Kirilyuk, P. A. Usachev, R. V. Pisarev, A. M. Balbashov, and T. Rasing, Ultrafast non-thermal control of magnetization by instantaneous photomagnetic pulses, Nature (London) **435**, 655 (2005).

[10] A. Kirilyuk, A. V. Kimel, and T. Rasing, Ultrafast optical manipulation of magnetic order, Rev. Mod. Phys. **82**, 2731 (2010).

[11] A. V. Kimel and M. Li, Writing magnetic memory with ultrashort light pulses, Nat. Rev. Mater. **4**, 189 (2019).

[12] Y. R. Shen, *The Principles of Nonlinear Optics* (Wiley, New York, 1984).

[13] J. P. van der Ziel, P. S. Pershan, and L. D. Malmstrom, Optically-Induced Magnetization Resulting from the Inverse Faraday Effect, Phys. Rev. Lett. **15**, 190 (1965).

[14] B. A. Zon, V. Y. Kupershmidt, G. V. Pakhomov, and T. T. Urazbaev, Observation of inverse Cotton-Mouton effect in the magnetically ordered crystal $(\mathrm{Lu},\mathrm{Bi})_3(\mathrm{Fe},\mathrm{Ga})_5\mathrm{O}_{12}$, JETP Lett. **45**, 272 (1987).

[15] T. Kampfrath, A. Sell, G. Klatt, A. Pashkin, S. Mährlein, T. Dekorsy, M. Wolf, M. Fiebig, A. Leitenstorfer, and R. Huber, Coherent terahertz control of antiferromagnetic spin waves, Nat. Photonics **5**, 31 (2011).

[16] S. Schlauderer, C. Lange, S. Baierl, T. Ebnet, C. P. Schmid, D. C. Valovcin, A. K. Zvezdin, A. V. Kimel, R. V. Mikhaylovskiy, and R. Huber, Temporal and spectral fingerprints of ultrafast all-coherent spin switching, Nature (London) **569**, 383 (2019).

[17] T. Satoh, Y. Terui, R. Moriya, B. A. Ivanov, K. Ando, E. Saitoh, T. Shimura, and K. Kuroda, Directional control of spin-wave emission by spatially shaped light, Nat. Photonics **6**, 662 (2012).

[18] J. A. De Jong, I. Razdolski, A. M. Kalashnikova, R. V. Pisarev, A. M. Balbashov, A. Kirilyuk, T. Rasing, and A. V. Kimel, Coherent Control of the Route of an Ultrafast Magnetic Phase Transition via Low-Amplitude Spin Precession, Phys. Rev. Lett. **108**, 157601 (2012).

[19] D. Afanasiev, B. A. Ivanov, A. Kirilyuk, T. Rasing, R. V. Pisarev, and A. V. Kimel, Control of the Ultrafast Photoinduced Magnetization across the Morin Transition in $DyFeO_3$, Phys. Rev. Lett. **116**, 097401 (2016).

[20] T. F. Nova, A. Cartella, A. Cantaluppi, M. Först, D. Bossini, R. V. Mikhaylovskiy, A. V. Kimel, R. Merlin, and A. Cavalleri, An effective magnetic field from optically driven phonons, Nat. Phys. **13**, 132 (2017).

[21] S. Baierl, M. Hohenleutner, T. Kampfrath, A. K. Zvezdin, A. V. Kimel, R. Huber, and R. V. Mikhaylovskiy, Nonlinear spin control by terahertz-driven anisotropy fields, Nat. Photonics **10**, 715 (2016).

[22] V. N. Gridnev, Phenomenological theory for coherent magnon generation through impulsive stimulated Raman scattering, Phys. Rev. B **77**, 094426 (2008).

[23] A. M. Kalashnikova, A. V. Kimel, R. V. Pisarev, V. N. Gridnev, P. A. Usachev, A. Kirilyuk, and T. Rasing, Impulsive excitation of coherent magnons and phonons by subpicosecond laser pulses in the weak ferromagnet $FeBO_3$, Phys. Rev. B **78**, 104301 (2008).

[24] D. Bossini, A. M. Kalashnikova, R. V. Pisarev, T. Rasing, and A. V. Kimel, Controlling coherent and incoherent spin dynamics by steering the photoinduced energy flow, Phys. Rev. B **89**, 060405(R) (2014).

[25] A. V. Kimel, R. V. Pisarev, J. Hohlfeld, and T. Rasing, Ultrafast Quenching of the Antiferromagnetic Order in $FeBO_3$, Phys. Rev. Lett. **89**, 287401 (2002).

[26] See Supplemental Material at http://link.aps.org/supplemental/10.1103/PhysRevLett.123.157202 for the detailed description of the experimental setup, $FeBO_3$ terahertz absorption spectrum, theoretical formulas for the q-FM and the q-AFM frequencies vs the external magnetic field, theoretical formalism of magnetization dynamics excitation and magnetization dynamics detection details, which includes Refs. [21,23,27–34].

[27] J. Hebling, G. Almasi, I. Kozma, and J. Kuhl, Velocity matching by pulse front tilting for large area THz-pulse generation, Opt. Express **10**, 1161 (2002).

[28] M. Sajadi, M. Wolf, and T. Kampfrath, Terahertz-field-induced optical birefringence in common window and substrate materials, Opt. Express **23**, 28985 (2015).

[29] M. Naftaly and R. E. Miles, Terahertz time-domain spectroscopy for material characterization, Proc. IEEE **95**, 1658 (2007).

[30] A. K. Zvezdin and A. A. Mukhin, New nonlinear dynamics effects in antiferromagnets (in Russian), Kratk. Soobshcheniya Po Fiz. FIAN **12**, 10 (1981).

[31] A. K. Zvezdin, A. I. Popov, and K. I. Turkmenov, The magnetooptical anisotropy of rare-earth crystals (in Russian). Fiz. Tver. Tela **28**, 1760 (1986).

[32] W. J. Tabor, A. W. Anderson, and L. G. Van Uitert, Visible and infrared faraday rotation and birefringence of single-crystal rare-earth orthoferrites, J. Appl. Phys. **41**, 3018 (1970).

[33] S. R. Woodford, A. Bringer, and S. Blügel, Interpreting magnetization from Faraday rotation in birefringent magnetic media, J. Appl. Phys. **101**, 053912 (2007).

[34] J. A. de Jong, A. M. Kalashnikova, R. V. Pisarev, A. M. Balbashov, A. V. Kimel, A. Kirilyuk, and T. Rasing, Effect of laser pulse propagation on ultrafast magnetization dynamics in a birefringent medium, J. Phys. Condens. Matter **29**, 164004 (2017).

[35] M. Pernet, D. Elmale, and J.-C. Joubert, Structure magnetique du metaborate de fer $FeBO_3$, Solid State Commun. **8**, 1583 (1970).

[36] G. Srinivasan and A. N. Slavin, *High Frequency Processes in Magnetic Materials* (World Scientific, Singapore, 1995).

[37] A. F. Andreev and V. I. Marchenko, Symmetry and the macroscopic dynamics of magnetic materials, Sov. Phys. Usp. **23**, 21 (1980).

[38] L. D. Landau and E. M. Lifshitz, *Electrodynamics of Continuous Media* (Pergamon, Oxford, 1984).

[39] L. D. Landau and E. M. Lifshitz, *Statistical Physics* (Pergamon, Oxford, 1970).

[40] G. A. Smolenskiĭ, R. V. Pisarev, and I. G. Siniĭ, Birefringence of light in magnetically ordered crystals, Sov. Phys. Usp. **18**, 410 (1975).

[41] A. M. Kalashnikova, A. V. Kimel, R. V. Pisarev, V. N. Gridnev, A. Kirilyuk, and T. Rasing, Impulsive Generation of Coherent Magnons by Linearly Polarized Light in the Easy-Plane Antiferromagnet $FeBO_3$, Phys. Rev. Lett. **99**, 167205 (2007).

[42] C. Tzschaschel, K. Otani, R. Iida, T. Shimura, H. Ueda, S. Günther, M. Fiebig, and T. Satoh, Ultrafast optical excitation of coherent magnons in antiferromagnetic NiO, Phys. Rev. B **95**, 174407 (2017).

[43] V. N. Polupanov, N. F. Dakhov, V. K. Kiselyev, and V. N. Seleznev, Investigation of iron borate on the submillimeter waves, Int. J. Infrared Millimeter Waves **16**, 1167 (1995).

[44] M. A. Popov, I. V. Zavislyak, H. L. Chumak, M. B. Strugatsky, S. V. Yagupov, and G. Srinivasan, Ferromagnetic resonance in a single crystal of iron borate and magnetic field tuning of hybrid oscillations in a composite structure with a dielectric: Experiment and theory, J. Appl. Phys. **118**, 013903 (2015).

[45] D. Afanasiev, I. Razdolski, K. M. Skibinsky, D. Bolotin, S. V. Yagupov, M. B. Strugatsky, A. Kirilyuk, T. Rasing, and A. V. Kimel, Laser Excitation of Lattice-Driven Anharmonic Magnetization Dynamics in Dielectric $FeBO_3$, Phys. Rev. Lett. **112**, 147403 (2014).

[46] R. V. Mikhaylovskiy, E. Hendry, A. Secchi, J. H. Mentink, M. Eckstein, A. Wu, R. V. Pisarev, V. V. Kruglyak, M. I. Katsnelson, T. Rasing, and A. V. Kimel, Ultrafast optical modification of exchange interactions in iron oxides, Nat. Commun. **6**, 8190 (2015).

[47] A. K. Zvezdin, Dynamics of domain walls in weak ferromagnets, JETP Lett. **29**, 553 (1979).

[48] J. A. Riordan and X.-C. Zhang, Sampling of free-space magnetic pulses, Opt. Quantum Electron. **32**, 489 (2000).

[49] L. V. Velikov, A. S. Prokhorov, E. G. Rudashevskiĭ, and V. N. Seleznev, Antiferromagnetic resonance in $FeBO_3$, Sov. Phys. JETP **39**, 909 (1974).